Fostering Sustainability through the Integration of Renewable Energy in ... Fostering Sustainability through the Integration of Renewable Energy in an Agricultural Hydroponic Greenhouse

Aymen Lachheb, Rym Marouani, Chabakata Mahamat, Safa Skouri, Salwa Bouadila

Fostering Sustainability through the Integration of Renewable Energy in an Agricultural Hydroponic Greenhouse

Aymen Lachheb
Laboratory Smart Electricity & ICT, SEICT, LR18ES44, National Engineering School of Carthage, University of Carthage, Tunisia
aymen.lachheb@enicarthage.rnu.tn (corresponding author)

Rym Marouani
Laboratory ATSSEE, Department of Physics, Faculty of Sciences de Tunis, University Tunis El Manar, Campus Universitaire Farhat Hached, Tunisia
rym.marouani@fst.utm.tn

Chabakata Mahamat
Universite de Guyane, UMR Espace-Dev, Cayenne, French Guiana, France
chabakata.mahamat@univ-guyane.fr

Safa Skouri
Centre de Recherches et des Technologies de l'Energie, Technopole de Borj-Cedria, Tunisia
skouri_safa@yahoo.fr

Salwa Bouadila
Centre de Recherches et des Technologies de l'Energie, Technopole de Borj-Cedria, Tunisia
salwa.bouadila@crten.rnrt.tn

Received: 21 January 2024 | Revised: 11 February 2024 | Accepted: 13 February 2024

 DOI: https://doi.org/10.48084/etasr.6939

ABSTRACT

This research explores the feasibility of integrating renewable energy sources, such as solar and wind, to power a hydroponic greenhouse. In this way, the latter's energy autonomy is ensured. The study begins by evaluating the annual electricity consumption of the examined system. A renewable energy system capable of meeting its energy requirements throughout the year is also designed. The main objective is to assess the efficiency of two types of renewable energy sources, namely photovoltaic panels and wind turbines, and to improve their integration within the agricultural chamber by implementing a model simulation. Two scenarios were examined: the first one represents a photovoltaic power plant with storage, connected to the grid, while the second scenario presents a wind power plant connected to the grid. This numerical analysis is supplemented by a one-year experimental study of a photovoltaic installation connected to the network with storage, which in turn is connected to the experimental device. To handle energy within the renewable energy greenhouse, an energy management system was developed based on a fuzzy logic controller. This system aims to maintain energy balance and ensure continuous power supply. The energy management system optimizes energy flow to minimize consumption, reduce grid dependence, and improve overall system efficiency, resulting in cost savings and certain environmental benefits.

Keywords-hydroponic greenhouse; PV installation; wind energy; energy management system; fuzzy logic control

I. INTRODUCTION

A notable increase in fossil fuel consumption has been detected across various sectors over the past few years, with Africa emerging as a growing influence in global energy trends, contributing to this boost in demand [1]. Recognizing the environmental challenges posed by the extended use of

fossil fuels, the region is highly expected to shift to renewable energy sources as a strategic solution to address this problem. This shift reflects a broader global effort to promote sustainable and environmentally friendly energy practices, highlighting the need for a transition to cleaner alternatives in the face of growing energy demand [2]. According to the International Renewable Energy Agency (IREA), there is a compelling projection that renewable energy will account for more than 60% of the world's total energy consumption by 2050, signifying a substantial move towards sustainable energy practices. This transition is already evident in the increasing contribution of solar and wind sources to electricity production, with a projected 17% growth compared to last year's 16%. In alignment with this global trend, the Tunisian Solar Plan has set ambitious targets for the year 2030. The plan aims to significantly enhance the country's renewable energy capacity by adding 3815 MW of installed power through various technologies. The distribution of this capacity includes 1510 MW for photovoltaic (PV) panels, 1755 MW for wind power generation, 450 MW for Concentrated Solar Power (CSP), and an additional 100 MW from power plants utilizing biomass resources. These targets underscore a comprehensive strategy to diversify the energy mix and embrace a more sustainable approach to meet growing energy demands while reducing dependence on fossil fuels. The concerted efforts outlined in both global and regional initiatives indicate a commitment to a cleaner, more resilient energy future.

Agrivoltaic systems, which combine PV energy production with agricultural activities on the same land, offer promising synergies for both sectors, potentially mitigating competition between energy and food production [3-6]. Authors in [7] combined PV panels, a hydrogen producer, and a ground source geothermal heat pump to heat a small greenhouse. The system offered an overall efficiency equal to 11%. Authors in [8] presented a simulation model analyzing solar radiation distribution within Mediterranean agrivoltaic greenhouses, a valuable tool for optimizing such systems. A hybrid system was proposed in [9] to analyze and predict zero energy potential in real-time air adaptation of direct PV systems for air conditioning of three regions in China. In [10], a system that incorporates both wind and heating is proposed, directly converting wind energy into thermal energy through water agitation heating in the greenhouse. In recent years, researchers have shown a strong interest in wind-resistant greenhouse designs [11-15]. A great amount of attention is also drawn in exploring methods for conditioning soilless technologies. The use of renewable energy in greenhouses demonstrates a great potential to reduce energy demand, operating costs, and CO_2 emissions [3, 5]. In many cases, significant amounts of energy are required to ensure the ideal growing conditions under greenhouses, posing major challenges for the greenhouse sector to eliminate energy demands while simultaneously improving the quality and quantity of the harvest [6]. Consequently, there is a crucial need to accelerate the further development and implementation of clean energy technologies to meet the challenges of the energy crisis and climate change [16].

This paper presents an improved approach to optimizing energy distribution in hydroponic greenhouses, aiming to enhance efficiency and sustainability. It introduces a control strategy encompassing two scenarios, designed to streamline energy distribution from various sources to successfully meet the greenhouse's electrical demands. The study begins with an overview of the components constituting the electrical energy system of a hydroponic greenhouse, followed by a detailed analysis to determine its annual energy demand. Subsequently, simulation assessments are performed to evaluate the integration of PV and wind systems into the intensified cropping system, guaranteeing that the latter aligns with the greenhouse's electrical requirements. An experimental investigation is also carried out to analyze the annual electricity consumption within the greenhouse.

II. ELECTRIC POWER REQUIRED IN HYDROPONIC GREENHOUSE

The hydroponic greenhouse is located on an experimental platform in Borj Cedria, Tunisia. Borj Cedria is situated on the northeastern coast of Tunisia in North Africa, approximately 25 km southeast of Tunis, at coordinates 36°41'34" N latitude and 10°24'39" longitude. Recognized for its coastal setting, Borj Cedria is a town within the greater Tunis metropolitan area. The experimental platform is equipped with a meteorological station enabling the measurement of various climatic parameters (maximum, minimum, and average) at 10-minute intervals. These parameters include wind speed, ambient temperature, and global solar irradiation. The northern region of Tunisia enjoys a Mediterranean climate, characterized by mild winters and hot and dry summers. The studied hydroponic greenhouse entails all the elements that guarantee an optimal environment for cultivation. Control of air temperature, airflow, water temperature, water circulation, and lighting are all incorporated into the design and can be fixed or vary depending on the needs of the vegetation. Table I illustrates the actuators installed in the hydroponic greenhouse. The experimental hydroponic greenhouse involves a comprehensive array of electrical equipment, encompassing ventilation and climate control devices, thermal conditioning systems (heating and cooling), lighting, and irrigation systems (Figure 1).

Fig. 1. Experimental hydroponic greenhouse.

TABLE I. ACTUATORS USED IN THE HYDROPONIC GREENHOUSE

Equipment	Water pump	Irrigation controller	Aerator	Speed variator	Fan type 1	Fan type 2	Centrifugal pump	Lamp	Acquisition chain
Units	1	1	2	1	2	1	1	8	1
Power (W)	80	10	60	900	250	50	370	16	20

The electrical energy consumption in a hydroponic greenhouse fluctuates throughout the year due to seasonal variations, operational needs, and vegetation requirements. For various operations (irrigation, ventilation, lighting, and thermal conditioning), the consumption varies between 0.75 and 2 kWh, with consumption being highest during peak load times. The consumption of the irrigation system shows a fluctuating pattern throughout the year, ranging between 25 and 165 Wh. As with lighting, the electricity consumption of the irrigation system is small compared to the total consumption of the greenhouse and does not exceed 0.16 kWh. The air conditioning systems remain the main electricity consumers.

III. ARCHITECTURE AND DESCRIPTION OF THE HYBRID POWER SYSTEM

Utilizing renewable energy sources to supply power hydroponic greenhouses represents a pivotal stride in the direction of sustainable agriculture. The effective integration and connection of these system components is imperative in order to guarantee a dependable and sustainable operation.

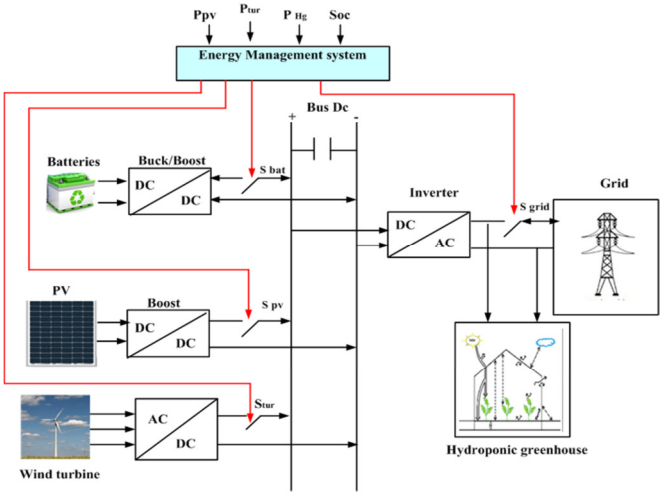

Fig. 2. Synoptic hydroponic greenhouse.

This research seeks to create a hybrid energy system connected to the grid and featuring an integrated battery storage system. The proposed design facilitates smooth grid connection/disconnection, effectively managing energy surplus or deficits. Incorporating this PV-battery system into a grid-connected hydroponic greenhouse can substantially decrease the reliance on grid energy, leading to environmental benefits, such as reduced CO_2 emissions and reduced bimonthly energy expenses. However, initial investment costs and dependence on weather conditions are potential challenges that require further consideration. Figure 2 outlines the proposed hybrid system architecture, with arrows indicating energy flow directions. This architecture serves as the foundation for this study. The proposed system comprises several components, including a renewable energy source (PV array or wind turbine generator) with a unidirectional DC/DC converter for Maximum Power Point Tracking (MPPT), a battery bank with a bidirectional DC/DC converter for managing the energy transfer between the battery and the DC bus, and a DC/AC inverter that facilitates energy exchange between the DC bus and the grid (see Figure 9). The setup ensures that the hybrid system can effectively deliver the necessary energy to fulfill the demands of the hydroponic greenhouse. The research delineates two scenarios:

- **Scenario 1:** PV/Battery/grid-connected power plant.
- **Scenario 2:** Wind turbine/ grid connected power plant.

A. PV-Battery -Grid-connected Power Plant Modeling

1) PV Power Plant Modeling

PV energy is widely recognized as the leading renewable power source. It holds a prominent position among renewable energy resources due to its eco-friendliness, abundance, and recyclability. In essence, a PV cell can be likened to an electrical current generator shunted with a diode. This diode is created through the formation of a p–n junction. To delve into the physical phenomena occurring within the cell, the model embodies two intrinsic resistors, *Rs* and *Rp*, in series and parallel arrangements [17-18]. Equation (1) describes the current (I_{pv}) generated by a PV module, which consists of several PV cells either connected in series or in parallel [1]. The current generated depends on the number of cells connected in series N_S and parallel N_P.

$$I_{pv} = N_p I_{pv} - N_p I_s \left[exp\left(\frac{V_{pv} + R_s I_{pv}}{nKTN_s} - 1\right)\right] - N_p Q \left[\frac{V_{pv} + R_s I_{pv}}{N_s R_p}\right] \quad (1)$$

where I_{pv} is the current generated by the PV panel, I_s is the saturation current of the diode, V_{pv} is the voltage generated by the panel, R_S is the cell series resistance, R_P is the cell parallel resistance, Q is the electron charge, n is the ideality diode factor (between 1 and 2), K is the Boltzmann constant, and T is the junction temperature. In this work, the FSM-300 W PV module was used. To ensure that the simulations provide accurate results and effectively visualize the performance of the PV power plant in relation to the available solar radiation, calculations were performed to determine the power generated. Power equation (2) can be expressed as a function of solar irradiation and ambient temperature [18]:

$$P_{pv}(t) = P_{pv(rated)}\left[1 + K(T_{amb} + (0.0256I(t)) - T_{ref}\right]\frac{I(t)}{I_{ref}} \quad (2)$$

where $P_{pv}(t)$ is the power generated by the PV panel at time t, $P_{pv\ (rated)}$ is the rated power of the PV panel, $I(t)$ is the solar irradiation at time t measured in W/m^2, I_{ref} is the reference solar irradiation (1000 W/m^2), T_{amb} is the ambient temperature and T_{ref} is the reference temperature (at 25 °C).

This scenario involves the study of a PV grid-connected power plant, where the proposed PV system is utilized to meet the energy demands of the hydroponic greenhouse. The hydroponic greenhouse energy requirements are primarily fulfilled by the PV system. If the power requirement is higher, additional energy is imported from the grid. The DC-DC converter is used to efficiently convert the DC voltage output from the PV modules to the voltage level required for the grid-connected inverter. The DC-DC converter boosts or bucks the voltage level depending on the specific needs of the grid-connected inverter and reassures that the MPPT algorithm is optimized for the operating conditions of the PV array. The DC-DC converter also improves the overall competence of the PV system by reducing power losses that can occur due to voltage mismatches between the PV panels and the grid-connected inverter.

MPPT is a technique to ensure that the PV system is operating at maximum efficiency and produces the maximum possible amount of energy under all operating conditions [19]. An MPPT algorithm is utilized to adjust the duty cycle (D) of the DC/DC converter. The duty cycle is the ratio of the on-time of a switch to the period of the waveform. By adjusting the duty cycle, the DC/DC converter voltage can be varied to track the Maximum Power Point (MPP) under all operating conditions. This signal is generated by a controller that monitors the output power of the PV array and compares it to the maximum power point. The controller then adjusts the duty cycle of the DC/DC converter to match the maximum power point.

The Perturb and Observe (P&O) algorithm is one of the most widely adopted techniques for achieving MPPT in PV systems. The P&O algorithm works by continually perturbing the operating point of the PV system and observing the resulting change in output power. In particular, the algorithm perturbs the duty cycle of the DC/DC converter by a small amount, typically 0.1%, and observes the resulting change in output power. Based on this observation, the algorithm adjusts the operating point of the PV system in the direction of power increase until it reaches the MPP of the system. The flowchart of the MPPT algorithm is provided in Figure 3.

2) Modeling of the Storage System

Energy Storage Systems (ESSs) play an important role in reducing the differences between energy production and consumption, which can be particularly difficult to manage when energy supplies rely on intermittent renewable sources, like wind and solar energy [20-22]. Batteries are among the most advanced electronic devices used to improve the robustness of smart electrical microgrids and store electrical energy. They are particularly valuable in addressing the inherent variability of renewable energy sources. In the field of battery modeling, numerous electrochemical models have been presented in the literature. These include models, such as the internal resistance battery model, the RC network battery model, and the Randles circuit. Among them, the Shepherd model is considered one of the most accurate models with corresponding electrical characteristics.

$$V_{bat} = E - R_{in} i_{bat} \tag{3}$$

$$E = E_0 - K\frac{Q}{Q - it} + Ae^{-Bit} \tag{4}$$

$$SOC(\%) = 100.(1 - \frac{Q_d}{C_{Bat}}) = 100.(1 - \frac{i_{Bat}}{C_{Bat}}t) \tag{5}$$

where E, V_{Bat}, i_{Bat}, Qd, and C_{Bat} are the battery electromotive force, the battery voltage, the battery current, ampere-hours stored, and the internal capacity, respectively.

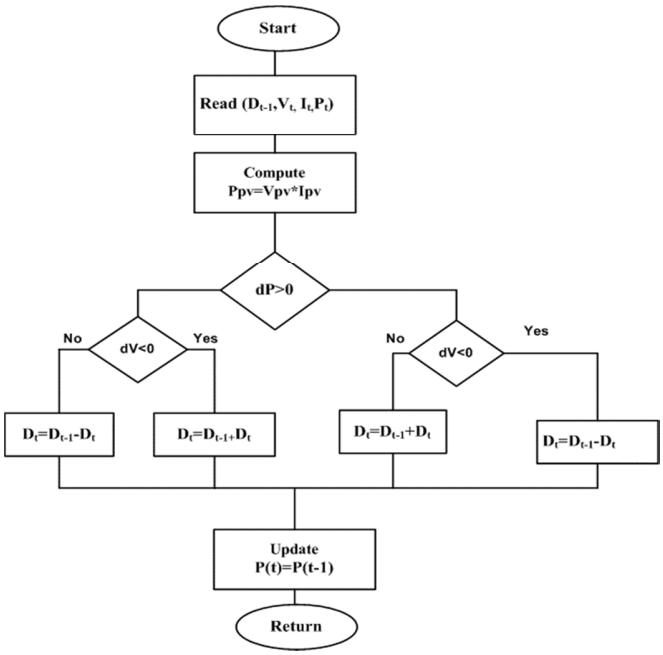

Fig. 3. Flowchart of the MPPT algorithm.

The Battery State Of Charge (SOC), representing the battery's stored electricity, is a crucial parameter for effective control. The proposed supervisory system must monitor the battery's SOC to make informed decisions based on its current state and the required power demand. Within the battery, the ampere-hours (Q_d) stored over a time interval (t) are related to the nominal battery capacity (C_{bat}) and the charging current (i_{Bat}). The hydroponic greenhouse is equipped with a lead-acid battery bank. Lead acid batteries are a prevalent choice in both off-grid and grid-connected PV systems. They are valued for their reliability, widespread global production, and cost-effectiveness in comparison to alternative PV storage technologies, like the lithium batteries. Additionally, lead-acid batteries offer several advantages, including low maintenance requirements, robust high current handling, suitability for deep

discharge conditions, favorable power density, and a wide operating temperature range. The battery bank consists of 16 cells with each cell having a capacity of 500 Ah and a nominal voltage of 24 V. Therefore, the total voltage of the battery bank is 48 V with a capacity of around 22 kWh. The battery is controlled through a bidirectional converter and a PI controller.

B. Energy Management based on Fuzzy Logic Control

The Fuzzy Logic Controller has emerged as one of the most effective tools in the scientific realm. This approach is distinguished by its straightforwardness and adaptability, drawing from theoretical advancements and human expert insights regarding the energy management of a hybrid system to power hydroponic greenhouses. These insights are employed to formulate fuzzy rules in the "if-then" linguistic format, all aimed at optimizing energy performance (Figure 4).

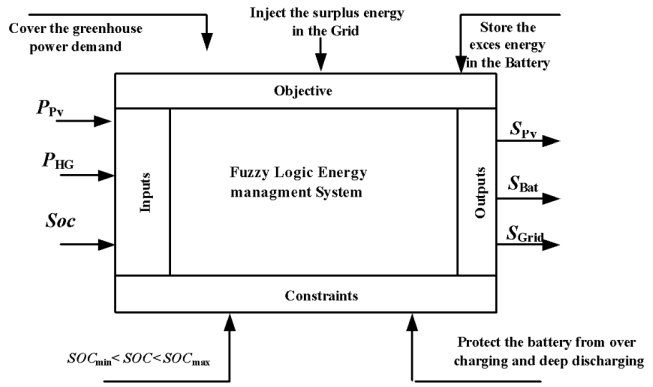

Fig. 4. Energy management system.

The fuzzy logic management algorithm consist of 3 inputs (P_{Pv}, P_{HG}, SOC) and 3 outputs (S_{pv}, S_{Bat}, S_{grid}), the management algorithm comprises three operating modes:

- Mode 1: The required energy of the load is covered through the PV installation.
- Mode 2: The required energy of the load is covered through batteries.
- Mode 3: The required energy of the load is covered through the grid.

To use the battery safely, two limits of the state of charge were defined: SOC_{min}=20% and SOC_{max}=80%. The management strategy should primarily use the power generated by the PV to satisfy the greenhouse load demand. Figure 5 illustrates the implementation of the proposed fuzzy logic controller engaging the Mamdani fuzzy inference system. This controller serves as the central decision-making hub for supplying the hydroponic greenhouse and charging batteries, ensuring they align with the specified conditions and operational requirements.

The principle of the fuzzy logic controller is based on generating three control signals S_{pv}, S_{Bat}, and S_{grid} starting from three inputs: PH Power (P_{pv}), greenhouse power demand (P_{HG}), and the battery state of charge SOC. S_{pv} is the control signal of the switch of the PV generators, S_{Bat} is the control signal of the battery switch, and S_{grid} is the control signal of the grid switch. Table II displays the rule table of a fuzzy controller where the inputs of the matrix are fuzzy sets of SOC, P_{pv} and P_{HG}. The output of this table is the state of the three switches S_{pv}, S_{Bat} and S_{grid}.

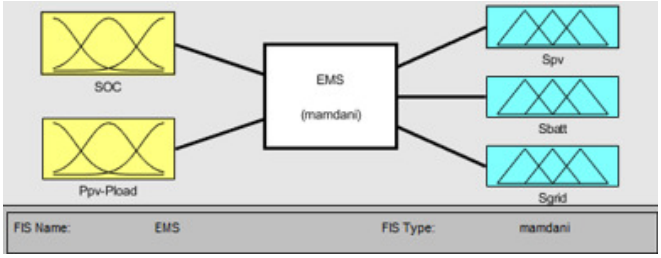

Fig. 5. EMS based on fuzzy logic controller.

TABLE II. DECISIONS MADE BY THE FUZZY LOGIC CONTROLLER.

G	$Ppv-P_{HG}$	SOC	S_{pv}	S_{Bat}	S_{Grid}	Decision
H	P	L	on	on	0	PVs supply HG and charge the battery
H	P	H	on	off	on	PVs supply HG and inject surplus energy to the grid
L	N	M	off	off	off	Battery supplies the HG
L	N	L	off	off	on	Grid supplies the HG

C. Simulation Results of the PV Power Plant

To verify the accuracy and effectiveness of the modeling and control techniques applied to the PV system that powers a hydroponic greenhouse, simulations were conducted using MATLAB software for both daily and annual periods.

1) Simulation Results of the PV Power Plant for One Day

Figure 6 illustrates the power output of the PV system, including the power supplied to the grid and the power demand of the hydroponic greenhouse. It exhibits the amount of electricity generated by the PV system during the simulation period. This information is crucial to understand the energy yield of the PV system and evaluate its performance. During the simulation period, it was observed that the power output of the PV array was zero between 00:00 Am and 05:00 Am and the grid supplied electricity during this period to meet the load demand. From the 5th hour, the PV system started to generate enough energy to cover the load demand. The grid reacted dynamically to the fluctuations in the load and the power of the PV system, thus ensuring that the entire energy requirement of the system was covered in the event of a production failure of the PV system. The excess energy from the PV system was fed into the grid. The simulation results presented in Figure 6 provide valuable insight into the performance and behavior of the PV system powering the hydroponic greenhouse. They demonstrate that the PV array can effectively meet the energy needs of the greenhouse and that the grid can be used as a backup power source when the PV array output fluctuates. The findings can be used to fine-tune the control strategy and improve system efficiency and reliability.

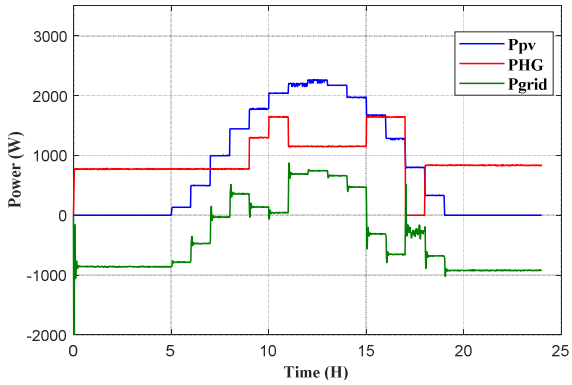

Fig. 6. Daily power generation from the PV system, grid supply, and hydroponic greenhouse power demand.

2) Simulation Results of the PV Power Plant for One Year

MATLAB was utilized to run simulations over a period of one year to experimentally validate the accuracy and efficacy of the modeling for the PV power plant. Figure 7 portrays the monthly electricity production of the PV system, the power supplied to the grid, and the power required by the hydroponic greenhouse. These values are strongly dependent on the solar radiation. In January, the PV system generated an average of 235 kWh. In May, the expected production was 358 kWh, indicating an increase of 52%. The highest production takes place in July with 370 kWh, const6ituting an increase of almost 58% compared to January. Figure 8 represents the percentage of PV system power generation for hydroponic greenhouse power demand and grid injection.

In the winter season, the power demand of the HG presented a percentage varying between 30% and 40% of the total electric energy generated by the PV system. During the summer season, the energy injected into the grid presented an average value of 85%. Thus, the designed PV system is able to meet the total hydroponic greenhouse electricity demand without considering energy storage systems.

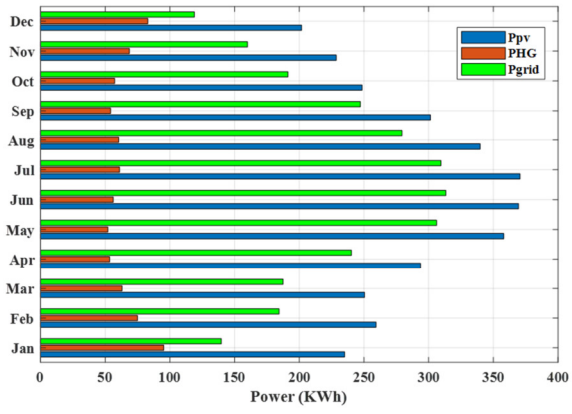

Fig. 7. Annual power generation from the PV system, grid supply, and hydroponic greenhouse power demand.

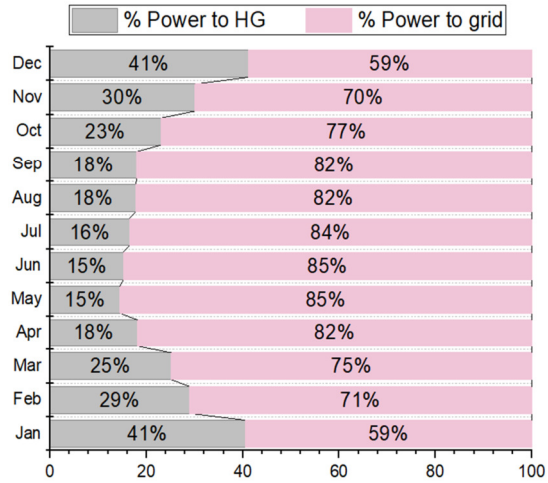

Fig. 8. Percentage of the PV system power generation for hydroponic greenhouse power demand and grid injection.

D. Wind Turbine Grid Connected Power Plant

1) Modeling

In this case, the aim is to create a wind turbine system for a hydroponic greenhouse that is connected to the electricity grid. To achieve this, the system is designed based on input data for the simulation, such as wind speed and direction, greenhouse location and orientation, energy demand profile and grid connection requirements. The main objective is to determine the ideal wind turbine specifications that will ensure consistent and efficient power generation for the greenhouse. This is accomplished by capturing the kinetic energy of the wind with aerodynamic blades, which in turn rotate the Permanent Magnet Synchronous Generator (PMSG) to produce electricity. The fundamental equation describing the mechanical power of the wind turbine is [23]:

$$P_{WT} = \frac{1}{2}\rho\pi R^2 V_{WT}{}^3 C_p(\lambda,\beta) \quad (6)$$

where P_{WT} is the mechanical power, ρ is the air density, R is the blade-radius, V_{WT} is the wind speed, and $C_p(\lambda,\beta)$ is the aerodynamic power coefficient which can be expressed as:

$$C_p(\lambda,\beta) = C_1\left(C_2\frac{1}{\lambda} - C_3\beta - C_4\right)e^{\frac{C_5}{\lambda_i}}$$
$$\frac{1}{\lambda_i} = \frac{1}{\lambda+0.08\beta} - \frac{0.035}{\beta^3+1} \quad (7)$$

where λ is the tip speed ratio, β is the blade pitch angle, $C_1 = 0.5$, $C_2 = 116$, $C_3 = 0.4$, $C_4 = 5$, and $C_5 = 21$.

When β is maintained constant, we can see that the power coefficient C_p has only one maximum value C_{p_max}, which corresponds to the optimal value of C_p [6]. Therefore, C_{p_max} can be expressed as:

$$\lambda = \frac{\omega_m R}{V_{WT}} \quad (8)$$

where ω_m is the mechanical angular velocity of the rotor.

The electrical properties of the PMSG can be expressed mathematically by [7]:

$$\begin{cases} u_d = R_S i_d + \dfrac{d(L_d i_d + \psi_m)}{dt} - w_e L_q i_q \\ u_q = R_S i_q + \dfrac{d(L_q i_q)}{dt} + w_e (L_d i_d + \psi_m) \end{cases} \quad (9)$$

where d and q are the synchronous rotating reference frame, R_S is the stator winding-resistance, w_e represents the electric pulsation, ψ_m is the generator rotor flux, i_d and i_q are the stator currents expressed in the $d-q$ reference frame, (L_d, L_q) and (u_d, u_q) are respectively the stator inductances and the stator voltages expressed in the $d-q$ reference frame.

The PMSG electromagnetic torque (T_e) can be calculated using the electromagnetic power (P_e) formula [25]:

$$P_e = w_m T_e = \frac{3}{2} w_e \left[(L_d i_d + \psi_m) i_q - L_q i_q i_d \right] \quad (10)$$

The active power and reactive power of a system can be calculated by [9]:

$$\begin{cases} P = u_d i_d + u_q i_q \\ Q = u_d i_q - u_q i_q \end{cases} \quad (11)$$

2) Simulation Results

Figure 12 depicts the MATLAB/Simulink schematic blocks of the wind turbine model. Wind turbine parameters are taken into consideration as inputs to the program. Such parameters are the wind speed and inclination angle, which are defined as variables or as constants. An AC/DC rectifier mainly converts the three-phase output into a single-phase output system. The main consumer is located between the wind power system and the connected grid, so that it can switch between them if necessary to supply the hydroponic greenhouse. The design configuration of this wind power system is shown below. The physical parameters of the proposed WTS are given in Table III.

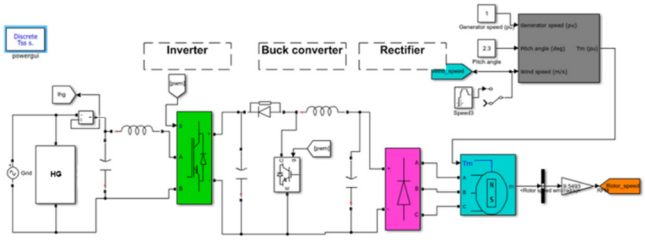

FIG. 9. Simulink assembly of the wind power system.

TABLE III. CHARACTERISTICS OF THE WIND TURBINE SYSTEM

Stator winding resistance of the PMSG (Ω)	0.18
Number of pole pairs	2
Moment of inertia (Kg/m^2)	0.0062
Armature inductance (H)	0.0835

One of the parameters characterizing the different models of wind turbines is the speed of rotation, which depends on wind speed. To compute the power of the wind turbine system, the wind speed is determined. In this study a wind turbine with a vertical axis of 1 kW is chosen. The recorded values for the minimum wind speed fluctuated between 0 and 4 m/s. The maximum value reached 10 m/s at noon. The average wind speed in north-west Tunisia varies between 0 and 6 m/s. Figure 10 demonstrates the daily electricity generation from the wind system, the grid supply, and the hydroponic greenhouse electricity demand. The presented numerical results disclose the electrical behavior of the wind system, which supplies the hydroponic greenhouse with an average value of about 500 W. They reveal that the wind generator can cover 50% of the energy needs of the greenhouse. The remainder of the electricity requirement is covered by the electricity grid. Compared to the first scenario, it becomes clear that the demand for electrical energy is covered more by PV than by wind turbines. The current generated at the output of the AC/DC/AC converter of the 1 kW vertical axis wind turbine is displayed in Figure 11. The current of the wind turbine only stabilizes when the wind speed is constant, which explains the fluctuations shown. Eventually, the wind speed stabilizes at the maximum value of 9 m/s, giving a maximum current of 11 A. The obtained simulation results indicate that the current has a sinusoidal shape, and the maximum amplitude varies according to the power requested by the hydroponic greenhouse load.

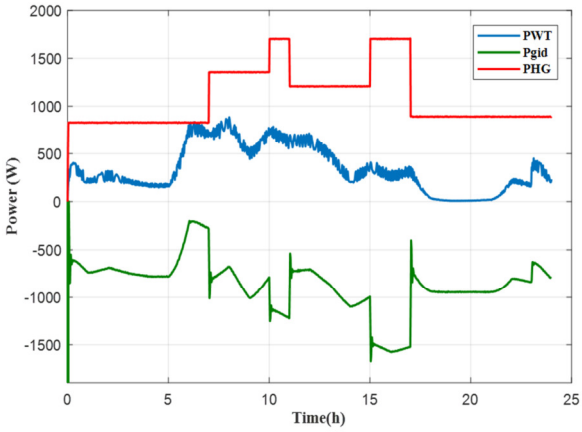

Fig. 10. Daily power generation from wind system, grid supply, and hydroponic greenhouse power demand.

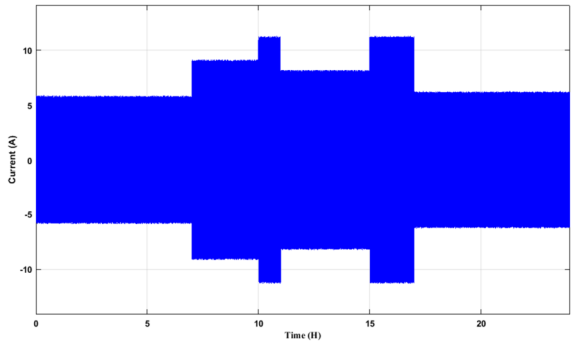

FIG. 11. Current generated by the wind grid-connected power plant.

The three-phase voltage generated by the proposed generator undergoes a conversion process that transforms it into single-phase voltage. This transformation is achieved through a rectifier and a single-phase inverter setup. The resulting output is maintained as AC voltage, with a maximum amplitude of 320 V. This voltage can supply the hydroponic greenhouse or be injected into the grid as per the requirements of the application. Figure 12 illustrates the relationship between the PMSG speed and the Wind Turbine System (WTS) electromagnetic torque. The rotor speed of the PMSG exhibits random fluctuations due to the variability in wind speed. Consequently, these fluctuations in the PMSG rotor speed result in corresponding changes in the electromagnetic torque and the power output of the generator.

The power created by a wind turbine as a function of turbine speed is described by its power curve at different wind speeds, as can be noticed in Figure 13. The generated turbine power is a polynomial curve. It depends on the parameters of wind speed and turbine speed. There are two significant turbine speeds: a maximum speed and a minimum speed at which the turbine produces the least power. The optimal speed is recorded when the turbine produces the maximum power, but this speed is variable according to the wind speed. For example, at a speed of 10 m/s, the turbine generates an optimal power of 1.2 kW.

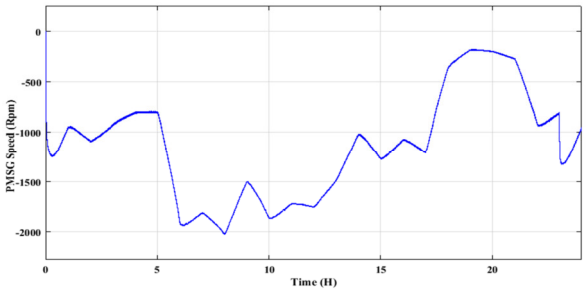

Fig. 12. Speed of the PMSG.

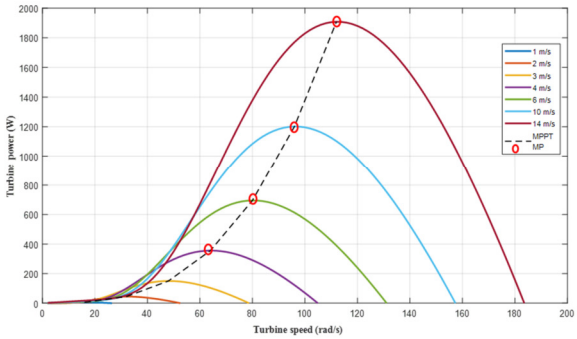

Fig. 13. Turbine power generated vs turbine speed for different wind speed values.

IV. IMPLEMENTATION AND EXPERIMENTAL VALIDATION OF THE PV - STORAGE SYSTEM

To design and optimize the performance of a PV system to supply a hydroponic greenhouse, various factors need to be considered during the design process. These include the available space for the solar panels, the orientation and angle of inclination of the panels, the location and climate of the site and the expected solar irradiation. Based on these factors, the solar panels, inverters, batteries, and cabling can be properly sized to ensure maximum efficiency and effectiveness of the system. After designing a grid-connected PV system to fulfill the electrical energy needs of the hydroponic greenhouse (as depicted in Figure 14), it was determined that the maximum power required by the greenhouse is 2 kW. Consequently, a 2.1 kWp PV system was selected to satisfy this demand.

Fig. 14. PV installation.

Fig. 15. Battery storing system.

To validate the numerical model, an experimental analysis has been performed over a year with an experimental PV system equipped with the HG layout. The scatter plots of the measured and predicted values of PV power and ambient temperature are portrayed in Figure 16. The latter underscores the effectiveness of the Simulink model developed in this study. With an ambient temperature of around 16 °C in winter and spring, the measured and predicted values showcased a slight difference. Figure 16 illustrates the generated and forecasted power, visualized as yearly variations over a 12-month period. A polynomial fit is applied to both the experimental and simulated data sets. The two polynomial fits have almost the same appearance with a slight variation, confirming the effectiveness of the developed Simulink model. In summer and autumn, the curves of the experimental and numerical results are almost identical.

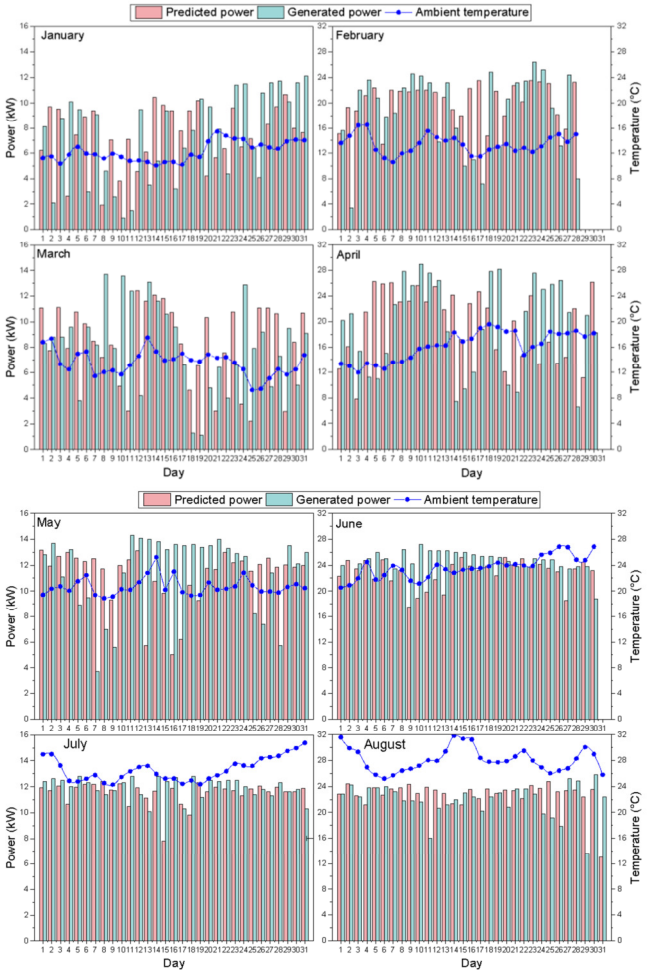

Fig. 16. Measured and predicted annual values of PV power and ambient temperature.

V. CONCLUSION

This study investigated the feasibility of implementing renewable energy systems, specifically solar and wind, to achieve the energy independence of a hydroponic greenhouse. The research was initiated with the design of a renewable energy system capable of fulfilling its energy requirements throughout the year. The efficiency of two renewable energy sources, photovoltaic panels and wind turbines has been demonstrated, and their integration within the agricultural chamber has been enhanced by using model simulations. Two scenarios were explored, each offering valuable insights into the optimization of energy management in renewable energy greenhouses. In the first scenario, the simulation results highlighted the dynamic behavior of the battery system, showcasing its resilience and reliability in addressing energy deficits during periods of low solar irradiation. The presented algorithm effectively optimized the combination of energy sources to minimize grid usage while maximizing photovoltaic cell utilization.

In the second scenario, it was observed that the wind turbine could cover 50% of the greenhouse's energy needs, indicating the superiority of photovoltaics compared to wind turbines in meeting the electrical energy demands. Furthermore, the numerical analysis was validated through a one-year experimental study on a grid-connected photovoltaic installation with storage, affirming the effectiveness of the Simulink model developed in this study.

In comparison to existing works, the current research provides valuable insights into sustainable and self-sufficient energy solutions for agricultural applications. By integrating renewable energy sources with advanced energy management systems, not only does this study contribute to reducing greenhouse gas emissions, but it also hilights the potential for efficient environmental regulation and resource utilization in hydroponic greenhouse operations.

REFERENCES

[1] W. Ahmed, J. A. Sheikh, A. Z. Kouzani, and M. A. P. Mahmud, "The Role of Single End-Users and Producers on GHG Mitigation in Pakistan—A Case Study," *Sustainability*, vol. 12, no. 20, Jan. 2020, Art. no. 8351, https://doi.org/10.3390/su12208351.

[2] F. Salata *et al.*, "Heading towards the nZEB through CHP+HP systems. A comparison between retrofit solutions able to increase the energy performance for the heating and domestic hot water production in residential buildings," *Energy Conversion and Management*, vol. 138, pp. 61–76, Apr. 2017, https://doi.org/10.1016/j.enconman.2017.01.062.

[3] S. Bouadila, S. Baddadi, S. Skouri, and R. Ayed, "Assessing heating and cooling needs of hydroponic sheltered system in mediterranean climate: A case study sustainable fodder production," *Energy*, vol. 261, Dec. 2022, Art. no. 125274, https://doi.org/10.1016/j.energy.2022.125274.

[4] S. Baddadi, S. Bouadila, W. Ghorbel, and A. Guizani, "Autonomous greenhouse microclimate through hydroponic design and refurbished thermal energy by phase change material," *Journal of Cleaner Production*, vol. 211, pp. 360–379, Feb. 2019, https://doi.org/10.1016/j.jclepro.2018.11.192.

[5] E. Cuce, D. Harjunowibowo, and P. M. Cuce, "Renewable and sustainable energy saving strategies for greenhouse systems: A comprehensive review," *Renewable and Sustainable Energy Reviews*, vol. 64, pp. 34–59, Oct. 2016, https://doi.org/10.1016/j.rser.2016.05.077.

[6] C. Lee, P. Hoes, D. Cóstola, and J. L. M. Hensen, "Assessing the performance potential of climate adaptive greenhouse shells," *Energy*, vol. 175, pp. 534–545, May 2019, https://doi.org/10.1016/j.energy.2019.03.074.

[7] A. S. Anifantis, A. Colantoni, and S. Pascuzzi, "Thermal energy assessment of a small scale photovoltaic, hydrogen and geothermal stand-alone system for greenhouse heating," *Renewable Energy*, vol. 103, pp. 115–127, Apr. 2017, https://doi.org/10.1016/j.renene.2016.11.031.

[8] F. A. Alturki, A. A. Al-Shamma'a, H. M. H. Farh, and K. AlSharabi, "Optimal sizing of autonomous hybrid energy system using supply-demand-based optimization algorithm," *International Journal of Energy Research*, vol. 45, no. 1, pp. 605–625, 2021, https://doi.org/10.1002/er.5766.

[9] C. Lu, S. Li, J. Gu, W. Lu, T. Olofsson, and J. Ma, "A hybrid ensemble learning framework for zero-energy potential prediction of photovoltaic direct-driven air conditioners," *Journal of Building Engineering*, vol. 64, Apr. 2023, Art. no. 105602, https://doi.org/10.1016/j.jobe.2022.105602.

[10] K. G. Tataraki, K. C. Kavvadias, and Z. B. Maroulis, "Combined cooling heating and power systems in greenhouses. Grassroots and retrofit design," *Energy*, vol. 189, Dec. 2019, Art. no. 116283, https://doi.org/10.1016/j.energy.2019.116283.

[11] A. Shaqour, H. Farzaneh, Y. Yoshida, and T. Hinokuma, "Power control and simulation of a building integrated stand-alone hybrid PV-wind-battery system in Kasuga City, Japan," *Energy Reports*, vol. 6, pp. 1528–1544, Nov. 2020, https://doi.org/10.1016/j.egyr.2020.06.003.

[12] F. Attig-Bahar, U. Ritschel, P. Akari, I. Abdeljelil, and M. Amairi, "Wind energy deployment in Tunisia: *Status, Drivers, Barriers and*

Research gaps—A Comprehensive review," *Energy Reports*, vol. 7, pp. 7374–7389, Nov. 2021, https://doi.org/10.1016/j.egyr.2021.10.087.

[13] S. Mahjoub, L. Chrifi-Alaoui, S. Drid, and N. Derbel, "Control and Implementation of an Energy Management Strategy for a PV–Wind–Battery Microgrid Based on an Intelligent Prediction Algorithm of Energy Production," *Energies*, vol. 16, no. 4, Jan. 2023, Art. no. 1883, https://doi.org/10.3390/en16041883.

[14] H. ur Rehman, J. Hirvonen, and K. Siren, "Influence of technical failures on the performance of an optimized community-size solar heating system in Nordic conditions," *Journal of Cleaner Production*, vol. 175, pp. 624–640, Feb. 2018, https://doi.org/10.1016/j.jclepro.2017.12.088.

[15] M. Ahliouati *et al.*, "Energetic and parametric studies of a basic hybrid collector (PV/T-Air) and a photovoltaic (PV) module for building applications: Performance analysis under El Jadida weather conditions," *Materials Science for Energy Technologies*, vol. 6, pp. 267–281, Jan. 2023, https://doi.org/10.1016/j.mset.2023.02.001.

[16] F. Wadie, "Evaluative analysis for standardized protection criteria against single and multiple lightning strikes in hybrid PV-wind energy systems," *Electric Power Systems Research*, vol. 218, May 2023, Art. no. 109227, https://doi.org/10.1016/j.epsr.2023.109227.

[17] D. Hidouri, R. Marouani, and A. Cherif, "Modeling and Simulation of a Renewable Energy PV/PEM with Green Hydrogen Storage," *Engineering, Technology & Applied Science Research*, vol. 14, no. 1, pp. 12543–12548, Feb. 2024, https://doi.org/10.48084/etasr.6492.

[18] N. Niveditha and M. M. Rajan Singaravel, "Optimal sizing of hybrid PV–Wind–Battery storage system for Net Zero Energy Buildings to reduce grid burden," *Applied Energy*, vol. 324, Oct. 2022, Art. no. 119713, https://doi.org/10.1016/j.apenergy.2022.119713.

[19] M. A. Abdullah, A. H. M. Yatim, C. W. Tan, and R. Saidur, "A review of maximum power point tracking algorithms for wind energy systems," *Renewable and Sustainable Energy Reviews*, vol. 16, no. 5, pp. 3220–3227, Jun. 2012, https://doi.org/10.1016/j.rser.2012.02.016.

[20] A. Sohani *et al.*, "Techno-economic evaluation of a hybrid photovoltaic system with hot/cold water storage for poly-generation in a residential building," *Applied Energy*, vol. 331, Feb. 2023, Art. no. 120391, https://doi.org/10.1016/j.apenergy.2022.120391.

[21] N. Arfaoui, S. Bouadila, and A. Guizani, "A highly efficient solution of off-sunshine solar air heating using two packed beds of latent storage energy," *Solar Energy*, vol. 155, pp. 1243–1253, Oct. 2017, https://doi.org/10.1016/j.solener.2017.07.075.

[22] A. Alanazi, "Optimization of Concentrated Solar Power Systems with Thermal Storage for Enhanced Efficiency and Cost-Effectiveness in Thermal Power Plants," *Engineering, Technology & Applied Science Research*, vol. 13, no. 6, pp. 12115–12129, Dec. 2023, https://doi.org/10.48084/etasr.6381.

[23] R. Ben Ali, H. Schulte, and A. Mami, "Modeling and simulation of a small wind turbine system based on PMSG generator," in *Evolving and Adaptive Intelligent Systems*, Ljubljana, Slovenia, Jun. 2017, pp. 1–6, https://doi.org/10.1109/EAIS.2017.7954833.

[24] E. N. F. Ltd, "ENF Ltd." https://fr.enfsolar.com/pv/panel-datasheet/crystalline/10249.

[25] S.-W. Lee and K.-H. Chun, "Adaptive Sliding Mode Control for PMSG Wind Turbine Systems," *Energies*, vol. 12, no. 4, Jan. 2019, Art. no. 595, https://doi.org/10.3390/en12040595.

[26] Y. Kassem, H. Camur, M. T. Adamu, T. Chikowero, and T. Apreala, "Prediction of Solar Irradiation in Africa using Linear-Nonlinear Hybrid Models," *Engineering, Technology & Applied Science Research*, vol. 13, no. 4, pp. 11472–11483, Aug. 2023, https://doi.org/10.48084/etasr.6131.